Introduction to Science Theme 3: multi-borehole observatory[1]

Kelemen, P.B., Matter, J.M., Teagle, D.A.H., Coggon, J.A., and the Oman Drilling Project Science Team[2]

Keywords: Oman Drilling Project, OmanDP, Samail ophiolite, Site BA1, Site BA2, Site BA3, Site BA4, batin alteration, multi-borehole observatory, Wadi Tayin massif, Wadi Laywani, Wadi Mehlah, mantle

Chapter contents

[1]Kelemen, P.B., Matter, J.M., Teagle, D.A.H., Coggon, J.A., and the Oman Drilling Project Science Team, 2021. Introduction to Science Theme 3: multi-borehole observatory. *In* Kelemen, P.B., Matter, J.M., Teagle, D.A.H., Coggon, J.A., and the Oman Drilling Project Science Team, *Proceedings of the Oman Drilling Project*: College Station, TX (International Ocean Discovery Program). https://doi.org/10.14379/OmanDP.proc.2020
[2]**OmanDP Science Team affiliations.**

MS OmanDP-114
Published 29 April 2021

Multi-borehole observatory (BA sites)

Selection of sites

The OmanDP "Batin Alteration"—BA drill sites, in actively weathering peridotite in the mantle section of the Wadi Tayin massif of the ophiolite, were chosen to create a "multi-borehole observatory" to study hydration, carbonation, and oxidation of exposed peridotite during near-surface weathering and the associated hydrogeological system, and to explore the subsurface chemosynthetic biosphere fostered by the weathering reactions. Cores collected at the BA sites will also be relevant for understanding mantle melt transport and in addressing the cooling history of the shallow mantle near a spreading ridge. Conversely, cores from the Crust-Mantle Transition Zone (CMTZ) drill Sites CM1A and CM2B (see the **Introduction to Science Theme 1B** chapter) in the Wadi Tayin massif, will shed further light on weathering, hydrogeology, and the subsurface biosphere in tectonically exposed peridotite.

Initially, we hoped to conduct drilling of actively altering peridotite in Wadi Dima, west of the present sites, in an area without large faults. However, we were not able to find drill sites more than 3.5 km from the nearest registered "falaj" (irrigation system) as required for permitting. Alternatives were (a) Wadi Laywani, a broad, south-facing drainage about 20 km northeast of the town of Batin and 4 km east of the road from the village of Batin to the village of Dima, and (b) the headwaters of Wadi Mehlah, along the Batin-Dima road. Wadi Mehlah is a long, straight north-northwest–trending valley north-northwest of Wadi Laywani, parallel to the Batin-Dima road, draining into Wadi Tayin east of the village of Mehlah in Wadi Dima, near its intersection with Wadi Tayin (Fig. **F1**).

Both of these alternative areas lie along a major northwest-southeast–trending fault system that cuts the Samail ophiolite (Fig. **F2**). An advantage of Wadi Laywani is that there has been prior sampling and analysis of groundwater and rock chips from water monitoring well NSHQ14 in that catchment (Mayhew et al., 2018; Miller et al., 2016; Paukert et al., 2012, 2019; Rempfert et al., 2017). The Oman Ministry of Regional Municipalities and Water Resources maintain this and other water monitoring wells.

Drilling in the BA area began with reconnaissance rotary boreholes in each of the two alternative areas in winter 2017. Hole BA1A is in Wadi Laywani. The water table was encountered at a depth of 13.5 m, and drill chips indicated that the bedrock was a mix of serpentinized dunite and harzburgite. Hole BA2A is in the headwaters of Wadi Mehlah. Surrounding outcrops and drill chips indicated that the hole is almost entirely in dunite. Other than the drilling fluid, there was essentially no water in Hole BA2A

within its full depth of 400 m (see **Note**, below). As a result, in order to ensure the presence of groundwater, we decided to drill all subsequent BA holes in Wadi Laywani.

Note. After completion of drilling, Hole BA2A was filled to a level of ~7 m below the surface using water (pH = 9.4) from a pool in a nearby wadi. After 15 min, the pH of water near the top of the Hole was 10.6. After 30 days, the water level in the Hole was 6.8 m. Geophysical logging of the hole showed that the hole was filled with alkaline, highly reduced water typical of peridotite-hosted alkaline springs in the Samail ophiolite.

Geology of the mantle section

The BA sites are entirely within partially serpentinized peridotite of the mantle section of the Samail ophiolite. Peridotites in the mantle section record at least one phase of extensive melting and melt-extraction, producing residual harzburgites. The harzburgites record about 20% melting, assuming the protolith had a fertile lherzolite composition.

In the northern massifs of the ophiolite, there are clear indications that there were two important stages of partial melting, melt transport, and magmatism, one during upwelling and corner flow in the shallow mantle beneath an oceanic spreading ridge and a later one producing crosscutting features. Products of this later stage are relatively rare in the southern massifs of the ophiolite, including Wadi Tayin and the neighboring Samail massif. For example, one characteristic of peridotites strongly affected by the later stage of melting is high Cr# (molar Cr/[Cr + Al]) in spinels, ranging 0.7–0.9 (e.g., Arai et al., 2006; Tamura and Arai, 2006, and references therein). By contrast, spinels in the southern massifs show a broad range of composition, with Cr# ranging 0.1–0.7 (e.g., Godard et al., 2000; Hanghøj et al., 2010; Monnier et al., 2006), similar to the range in peridotites dredged from the mid-ocean ridges (Dick and Bullen, 1984), and do not extend to higher values.

The BA sites lie within the mantle section of the Wadi Tayin massif of the Samail ophiolite. This is one of the largest and most intact massifs in the ophiolite. A well-exposed crustal section in the "Ibra syncline," about 7 km thick from seafloor pillow lavas to the CMTZ, has been the subject of many detailed studies (e.g., papers in Coleman and Hopson, 1981; Coogan et al., 2006; France et al., 2009; Garrido et al., 2001; Müller et al., 2017; Oeser et al., 2012; VanTongeren et al., 2015, 2008). OmanDP Holes GT1A and GT2A, drilled in winter 2017, sampled lower crustal gabbros in this section. The Mantle Transition Zone (MTZ) of the Wadi Tayin massif is exposed in outcrop in several places, including Wadi Nassif and nearby Wadi Zeeb (Fig. **F1**). The latter was the site of Holes CM1A, CM1B, CM2A, and CM2B in late fall 2017, which provided a complete section through the transition zone. The MTZ dips 20°–30° south-southwest along the strike length of the Wadi Tayin massif (Bailey, 1981; Nicolas et al., 2000). If there has been no tectonic thinning or thickening, then the structural thickness of the mantle section extends 10–20 km below the base of the crust.

The MTZ and surrounding crust and mantle are cut and displaced by several kilometers along a set of north-northwest–trending strike-slip faults (Fig. **F2**). Perhaps related to these smaller features, a 10 km scale north-northwest–trending fault system cuts all the way across the Wadi Tayin massif in Wadi Laywani (draining south) and Wadi Mehlah (draining north). The sense of displacement along this larger fault system has not been determined, but it is possible that it too is a right-lateral strike-slip fault.

At least one of the strike-slip faults, along Wadi Khafifah, continues as a ductile shear zone extending several kilometers into the mantle section (Nicolas and Boudier, 2008). Along this shear zone, deformation was localized in gabbroic dikes within the mantle (Homburg et al., 2010). Strongly deformed gabbroic dikes are observed in outcrop in the vicinity of the BA sites. Ductile deformation of the dikes may be related to movement along the large fault system; if so, the faults became active while the mantle section of the Wadi Tayin massif was still at high temperature, though deformation clearly continued into the low-temperature, brittle regime.

Normally, Samail ophiolite peridotites have foliation that is approximately parallel to the MTZ and the paleoseafloor (e.g., synoptic cross-sections in Lippard et al., 1986; Nicolas et al., 1988). A peculiar structural relationship has been observed—but rarely documented in publications—across parts of the Wadi Tayin mantle section, in which peridotite foliation is steep with respect to the shallow dip of the MTZ (e.g., Boudier and Coleman, 1981, their figure 2), while spinel lineation in the peridotite foliation has a low dip, approximately parallel to that of the MTZ. Perhaps fortunately, indications from surface mapping and drill site observation of core are that peridotite foliation at the BA sites has a shallow dip, approximately parallel to the MTZ exposed in east-facing outcrops on ridges forming the west side of Wadi Laywani, southwest of Site BA3. However, the odd geometry of foliation and lineation further west in the Wadi Tayin is important to note and may be important in syntheses of drilling results and surface observations.

Geological mapping in the late 1970s identified two particularly large dunite bodies in the Wadi Tayin mantle section, within depleted residual mantle harzburgite (Bailey, 1981). The dunites dip 20°–30° south-southwest, approximately parallel to the overlying MTZ. Kelemen et al. (2000, their table 1) measured the thickness of the northeastern dunite body,

perpendicular to top and bottom contacts with harzburgite, to be ~70 m, in the range of other large mantle dunites. More extensive size-frequency data on mantle dunites are reported by Braun and Kelemen (2002).

Unpublished observations by Peter Kelemen, and later by Bob Miller established the south-southwest dip of the southwestern dunite body at its thin northwestern tip, where it is ~2 km below the MTZ. However, there have been no estimates of its thickness in its central region, near Site BA2, due to faulting and irregular contacts. Also unpublished is the observation that between the two large, south-southwest–dipping dunites in a zone parallel to the Batin–Dima road, is a set of thinner dunites, up to 20 m wide, with steep north-northeast dips (Fig. **F3**). One potential explanation for these relationships, with shallow dunites to the southwest and northeast flanking a central zone of steeply dipping dunites, is that the central dunites represent a frozen zone of mantle upwelling beneath a ridge, while the MTZ-parallel dunites to the northeast and southwest have been transposed by corner flow on either side of the ridge. However, given that the Wadi Tayin massif is faulted and folded to the east, where it is overlain by Late Cretaceous to Miocene limestones, it is not clear whether features within the massif retain their structural orientation, with respect to each other and to the CMTZ, or not.

Sites BA2 and BA4 lie within the outcrop of the southeastern tip of the large, shallowly south-southwest–dipping dunite body. On site observations of drill cuttings (Fig. **F1** in the **Site BA2** chapter) indicate that the entire 400 m Hole BA2A is within massive dunite. Assuming a southwest dip of 25°–30°, parallel to the MTZ, this indicates that the dunite at Site BA2A is more than 350 m thick perpendicular to the MTZ. As such, it is more than three times thicker than the next thickest dunite in the mantle section of the Samail ophiolite, as measured by Kelemen et al. (2000, their table 1).

Holes BA1A, BA1B, and BA1D intersected the same large dunite body where it is ~100 m thick and ~3 km structurally beneath the MTZ to the south. The large dunite may (or may not) extend across Wadi Laywani, where a few relatively thin south-southwest–dipping dunite lenses can be seen on west-southwest–facing outcrops (Fig. **F2B**).

Dunites in the mantle section of ophiolites—and by inference in the mantle beneath oceanic spreading ridges—are generally understood to be the products of reaction between olivine-saturated melt—ascending by porous flow along crystal grain boundaries—and shallow mantle harzburgites. Orthopyroxene from the harzburgite dissolves, producing olivine + melt, and this leads to formation of dunites in channels of focused porous flow. Typically, olivine in mantle dunites has about the same composition (Mg#, molar Mg/[Mg + Fe], ~0.91) as in the surrounding harzburgites, consistent with formation of dunite by reaction rather than as the residue of extensive partial melting and melt extraction (Benoit et al., 1999; Rospabé et al., 2017) or as newly crystallized magmatic rocks.

As melt approaches the surface and begins to cool, it will begin to undergo crystallization and accompanying chemical fractionation, potentially producing olivine with a lower Mg#. If it continues to react with mantle peridotite, open-system processes will buffer the composition of cooling melt to various degrees in a process termed "reactive fractionation" (Abily and Ceuleneer, 2013; Collier and Kelemen, 2010). Other more complex processes in the uppermost mantle have also been proposed (Rospabé et al., 2018). Given the proximity of the large dunite at Sites BA1, BA2, and BA4 to the MTZ, it will be interesting to see if it records reactive fractionation, or even more complex open-system processes.

Cutting the dunite around the BA sites are numerous tabular gabbroic dikes and pyroxenite dikes. Though this has not been quantified, it is clear that the dikes are significantly more numerous than is typical in the mantle section of the Samail ophiolite. The dikes range from fine grained to pegmatoidal and may be an important source of calcium during alteration and weathering of the peridotite.

It is not clear why there is an unusual dike swarm in the vicinity of the BA sites. However, the presence of dikes in the mantle section of the Samail ophiolite is common. A late set of gabbronorite and websterite dikes cutting mantle peridotite foliation and dunite contacts occurs throughout the ophiolite. Geochemical characteristics of these dikes indicate that they are not related to the magmas that formed the overlying crust and could be formed from small amounts of late, shallow melts of residual mantle harzburgite (Kelemen et al., 1997). Less commonly (but not far away, in the Samail massif of the ophiolite), there are also olivine gabbro and troctolite dikes in the mantle, which could have crystallized from the same kind of magmas that formed the crust (Ceuleneer et al., 1996). It is not yet clear which kinds of lithologies predominate in the dike swarm around the BA sites.

Emplacement of the ophiolite and the underlying, allochthonous Hawasina Formation onto the Arabian continental margin followed subaerial weathering of the ophiolite was complete by about 74 Ma. Extensive erosion of the eastern part of the Wadi Tayin massif exposed mantle peridotite at the surface, locally forming laterites in a discontinuous band that extends to ~ km east of Sites BA1, BA3, and BA4 (Al Khirbash, 2015). After a Late Cretaceous marine transgression, latest Cretaceous and Tertiary shallow-water sediments were deposited unconformably on the peridotites in this area (Alsharan and Nasir,

1996; Hansman et al., 2017; Nolan et al., 1990). It is not clear how much of the low-temperature alteration of the peridotite in the multi-borehole observatory may have occurred during these episodes and how much is related to more recent weathering.

Groundwater composition and hydrogeology in the mantle section of the ophiolite has been a subject of fairly extensive research (Canovas et al., 2017; Chavagnac et al., 2013a, 2013b; Dewandel et al., 2005, 2004; Falk et al., 2016; Leleu et al., 2016; Mayhew et al., 2018; Mervine et al., 2014, 2015; Miller et al., 2016; Neal and Stanger, 1985; Noël et al., 2018; Paukert et al., 2012; Rempfert et al., 2017; Streit et al., 2012). As described in a classic paper about peridotite-hosted springs in California (Barnes and O'Neil, 1969), groundwater in peridotite catchments in Oman can be divided into two types. $MgHCO_3$-rich "Type 1" waters with pH ~8–9 are common in pools and running water in wadis and in most shallow wells. These waters are thought to be produced by near-surface weathering of the peridotite, dissolving Mg^{2+}, together with uptake of CO_2 from the atmosphere to form bicarbonate.

End-member $Ca(OH)_2$-rich "Type 2" waters have pH > 11 and are generally restricted to alkaline springs with associated travertine deposits and some deeper wells in peridotite. These waters are thought to form via more extensive, perhaps deeper interaction between groundwater and peridotite. Mg and CO_2 are lost, due to precipitation of serpentine and carbonate minerals, while Ca^{2+} is dissolved along the flow path. The source of Ca^{2+} could be the peridotite (e.g., Barnes and O'Neil, 1969), gabbro, and pyroxenite dikes (Streit et al., 2012), and/or calcium-carbonate minerals formed during earlier alteration (Noël et al., 2018).

Both Type 1 and Type 2 waters, and apparent mixtures of the two, are present in Wadi Laywani. Prior to OmanDP, the presence of Type 2 waters in monitoring well NSHQ14 was known. Water sampling and geophysical logging of Hole BA1A, drilled in 2017, established that Type 1 waters were also present, particularly at shallow depths (<60 m), together with relatively fresh, pH 6–8 water at the top of the hole, probably representing less modified, recent rain water.

In general, Oman mantle peridotite compositions are slightly displaced toward lower Mg/Si compared to inferred and experimentally observed residues of partial melting and the composition of residual peridotites dredged from mid-ocean ridges (e.g., Monnier et al., 2006, their figure 5). This is most evident where peridotites are strongly weathered and could be due to magnesium extraction (Snow and Dick, 1995) or to silicon addition (e.g., de Obeso and Kelemen, 2018). It will be interesting to observe the extent to which Mg/Si is low in peridotites in drill cores from Wadi Laywani. Large extents of Mg extraction should be evident in shifts to lower Mg/Fe as well as Mg/Si. Analysis of relict olivine, compared to bulk rock analyses, may offer an opportunity to discern whether Mg/Fe has been shifted due to weathering.

Geochemistry on drill cuttings

XRD analysis at Southampton University

Cuttings from rotary Holes BA1A and BA2A were analyzed by XRD at Southampton University School of Ocean and Earth Science XRD Laboratory. X-ray diffractograms were produced for each sample; a summary of results is shown in Table T1.

XRF analysis at Plymouth University

XRF analysis was used to determine major oxides and trace elements of 6 samples from rotary Holes BA1A and BA2A (3 samples from each hole) using milled drill cuttings samples from different depth intervals. Results are shown in Table T2.

XRF analysis at Sultan Qaboos University

XRF analyses of cuttings at 10 m intervals were made at Sultan Qaboos University (SQU) for rotary-drilled Holes BA1C, BA1D, CM1B, and CM2A. These data are imprecise and inaccurate, and some values are entirely incorrect (e.g., SiO_2 concentrations < 30% and > 70%), whereas other values may perhaps have been attributed to the wrong element. Table T3 compares SQU analyses of three standards (two peridotites and one Mg-rich basalt) with community accepted values and illustrates working curves, based on these data for elements with a systematic difference between SQU and community values, that can be used to correct the SQU analyses.

Table T4 presents SQU analyses of drill cuttings from Holes BA1C, BA1D, CM1B, and CM2A together with approximate CIPW norms for these data. Four options are presented: (1) "SQU quantitative analyses" without correction, (2) "Corrected quantitative analyses," (3) "SQU semiquantitative analyses" without correction, (4) "Corrected semiquantitative analyses." Corrected analyses used the working curves from Table T3. In general, these data add little to our understanding of the lithologies in the cuttings from the rotary drilled holes.

References

Abily, B., and Ceuleneer, G., 2013. The dunitic mantle-crust transition zone in the Oman ophiolite: Residue of melt-rock interaction, cumulates from high-MgO melts, or both? Geology, 41:67-70.

Al Khirbash, S., 2015. Genesis and mineralogical classification of Ni-laterites, Oman Mountains. Ore Geol. Rev., 65:199-212.

Alsharan, A.S., Nasir, S.J.Y., 1996. Sedimentological and geochemical interpretation of a transgressive sequence: the Late Cretaceous Oahlah Formation in the western Oman Mountains, United Arab Emirates. Sedimentary Geol., 101:227-242.

Arai, S., Kadoshima, K., Morishita, T., 2006. Widespread arc-related melting in the mantle section of the northern Oman ophiolite as inferred from detrital chromian spinels. J. Geol. Soc. London, 163:869-879.

Bailey, E.H., 1981. Geologic map of Muscat-Ibra area, Sultanate of Oman. J. Geophys. Res., 86.

Barnes, I., O'Neil, J.R., 1969. Relationship between fluids in some fresh alpine-type ultramafics and possible modern serpentinization, western United States. GSA Bull., 80:1947-1960.

Benoit, M., Ceuleneer, G., Polvém M., 1999. The remelting of hydrothermally altered peridotite at mid-ocean ridges by intruding mantle diapirs. Nature, 402:514-518.

Boudier, F., Coleman, R.G., 1981. Cross section through the peridotite in the Semail ophiolite. J. Geophys. Res., 86:2573-2592.

Braun, M.G., Kelemen, P.B., 2002. Dunite distribution in the Oman ophiolite: Implications for melt flux through porous dunite conduits. Geochem., Geophys., Geosyst., 3.

Canovas, P.A., Hoehler, T., Shock, E.L., 2017. Geochemical bioenergetics during low-temperature serpentinization: An example from the Samail ophiolite, Sultanate of Oman. J. Geophys. Res., Biogeosci., 122:1821–1847.

Ceuleneer, G., Monnereau, M., Amri, I., 1996. Thermal structure of a fossil mantle diapir inferred from the distribution of mafic cumulates. Nature, 379:149-153.

Chavagnac, V., Ceuleneer, G., Monnin, C., Lansac, B., Hoareau, G., Boulart, C., 2013a. Mineralogical assemblages forming at hyperalkaline warm springs hosted on ultramafic rocks: a case study of Oman and Ligurian ophiolites. Geochem., Geophys., Geosyst., 14:2474-2495.

Chavagnac, V., Monnin, C., Ceuleneer, G., Boulart, C., Hoareau, G., 2013b. Characterization of hyperalkaline fluids produced by low-temperature serpentinization of mantle peridotites in the Oman and Ligurian ophiolites. Geochem., Geophys., Geosyst., 14:2496-2522.

Coleman, R.G., Hopson, C.A. (Eds.), 1981. Oman Ophiolite Special Issue. J. Geophys. Res., 86:2495-2782.

Collier, M.L., Kelemen, P.B., 2010. The Case for Reactive Crystallization at Mid-Ocean Ridges. J. Petrol., 51:1913-1940.

Coogan, L.A., Howard, K.A., Gillis, K.M., Bickle, M.J., Chapman, H., Boyce, A.J., Jenkin, G.R.T., Wilson, R.N., 2006. Chemical and thermal constraints on focused fluid flow in the lower oceanic crust. Am. J. Sci., 306:389-427.

de Obeso, J.C., Kelemen, P.B., 2018. Fluid rock interactions in residual mantle peridotites overlain by shallow oceanic limestones: Insights from Wadi Fins, Sultanate of Oman. Chem. Geol., 498:139-149.

Dewandel, B., Lachassagne, P., Boudier, F., Al-Hattali, S., Ladouche, B., Pinault, J.-L., Al-Suleimani, Z., 2005. A conceptual hydrogeological model of ophiolite hard-rock aquifers in Oman based on a multiscale and a multidisciplinary approach. Hydrogeology J., 13:708-726.

Dewandel, B., Lachassagne, P., Qatan, A., 2004. Spatial measurements of stream baseflow, a relevant method for aquifer characterization and permeability evaluation: Application to a hard-rock aquifer, the Oman opholite. Hydrol. Process., 18:3391-3400.

Dick, H., Bullen, T., 1984. Chromian spinel as a petrogenetic indicator in abyssal and alpine-type peridotites and spatially associated lavas. Contrib. Mineral. Petrol., 86:54-76.

Falk, E.S., Guo, W., Paukert, A.N., Matter, J.M., Mervine, E.M., Kelemen, P.B., 2016. Controls on the stable isotope compositions of travertine from hyperalkaline springs in Oman: Insights from clumped isotope measurements. Geochim. Cosmochim. Acta, 192:1-28.

France, L., Ildefonse, B., Koepke, J., 2009. Interactions between magma and hydrothermal system in Oman ophiolite and in IODP Hole 1256D: Fossilization of a dynamic melt lens at fast spreading ridges. Geochem., Geophys., Geosyst., 10.

Garrido, C.-J., Kelemen, P.B., Hirth, G., 2001. Variation of cooling rate with depth in lower crust formed at an oceanic spreading ridge: Plagioclase crystal size distributions in gabbros from the Oman ophiolite. Geochem., Geophys., Geosyst., 2:2000GC000136.

Godard, M., Noël, J., Martinez, I., Williams, M., Escario, S., Oliot, E., Boudier, F., 2019. Linkages between serpentinization and carbon trapping in the Oman ophiolite: Evidence from the Wadi Dima and Batin peridotites. Goldschmidt Abstract 1159, Goldschmidt Conference, Barcelona, Spain, 18-23 Aug. 2019.

Godard, M., Jousselin, D., Bodinier, J.-L., 2000. Relationships between geochemistry and structure beneath a palaeo-spreading centre: A study of the mantle section in the Oman ophiolite. Earth Planet. Sci. Lett., 180:133-148.

Hanghøj, K., Kelemen, P., Hassler, D., Godard, M., 2010. Composition and genesis of depleted mantle peridotites from the Wadi Tayin massif, Oman ophiolite; Major and trace element geochemistry, and Os isotope and PGE systematics. J. Petrol., 51:201-227.

Hansman, R.J., Ring, U., Thomson, S.N., den Brok, B., Stübner, K., 2017. Late Eocene uplift of the Al Hajar Mountains, Oman, supported by stratigraphy and low-temperature thermochronology. Tectonics, 36:3081-3109.

Homburg, J., Hirth, G., Kelemen, P.B., 2010. Investigation of the strength contrast at the Moho: A case study from the Oman Ophiolite. Geology, 38:679-682.

Kelemen, P.B., Braun, M., Hirth, G., 2000. Spatial distribution of melt conduits in the mantle beneath oceanic spreading ridges: Observations from the Ingalls and Oman ophiolites. Geochem., Geophys., Geosyst., 1. https://doi.org/10.1029/999GC000012

Kelemen, P.B., Hirth, G., Shimizu, N., Spiegelman, M., Dick, H.J.B., 1997. A review of melt migration processes in the adiabatically upwelling mantle beneath oceanic spreading ridges. Phil. Trans. Roy. Soc. London A, 355:283-318.

Leleu, T., Chavagnac, V., Delacour, A., Noiriel, C., Ceuleneer, G., Aretz, M., Rommevaux, C., Ventalon, S., 2016. Travertines associated with hyperalkaline springs: Evaluation as a proxy for paleoenvironmental conditions, and sequestration of atmospheric CO_2. J. Sedimentary Res., 86:1328-1343.

Lippard, S.J., Shelton, A.W., Gass, I.G., 1986. The Ophiolite of Northern Oman. Geol. Soc. Lond. Mem., 11.

Mayhew, L.E., Ellison, E.T., Miller, H.M., Kelemen, P.B., Templeton, A.S., 2018. Iron transformations during low temperature alteration of variably serpentinized rocks from the Samail ophiolite, Oman. Geochim. Cosmochim. Acta, 222:704-728.

Mervine, E.M., Humphris, S.E., Sims, K.W.W., Kelemen, P.B., Jenkins, W.J., 2014. Carbonation rates of peridotite in the Samail Ophiolite, Sultanate of Oman constrained through ^{14}C dating and stable isotopes. Geochim. Cosmochim. Acta, 126:371-397.

Mervine, E.M., Sims, K.W.W., Humphris, S.E., Kelemen, P.B., 2015. Applications and limitations of U-Th disequilibria systematics for determining rates of peridotite carbonation in the Samail Ophiolite, Sultanate of Oman. Chem. Geol., 412:151-166.

Miller, H.M., Matter, J.M., Kelemen, P., Ellison, E.T., Conrad, M., Fierer, N., Templeton, A.S., 2016. Modern water/rock reactions in Oman hyperalkaline peridotite aquifers and implications for microbial habitability. Geochim. Cosmochim. Acta, 179:217-241.

Monnier, C., Girardeau, J., Le Mée, M.P., 2006. Along-ridge petrological segmentation of the mantle in the Oman ophiolite. Geochim. Cosmochim. Acta, 7. https://doi.org/10.1029/2006GC001320

Müller, T., Koepke, J., Garbe-Schönberg, C.D., Dietrich, M., Bauer, U., Wolff, P.E., 2017. Anatomy of a frozen axial melt lens from a fast-spreading paleo-ridge (Wadi Gideah, Oman ophiolite). Lithos, 272:31-45.

Neal, C., and Stanger, G., 1985. Past and present serpentinization of ultramafic rocks: An example from the Semail ophiolite nappe of northern Oman. In Drewer, J.I. (Ed.), The Chemistry of Weathering: Holland (D. Reidel Publ. Co.), 249-275.

Nicolas, A., and Boudier, F., 2008. Large shear zones with no relative displacement. Terra Nova, 20:200-205.

Nicolas, A., Boudier, F., Ildefonse, B., Ball, E., 2000. Accretion of Oman and United Arab Emirates ophiolite: Discussion of a new structural map. Marine Geophys. Res., 21:147-179.

Nicolas, A., Reuber, I., Benn, K., 1988. A new magma chamber model based on structural studies in the Oman ophiolite. Tectonophys., 151:87-105.

Noël, J., 2018. Etude pétro-structurale et géochimique des processus de serpentinisation et carbonatation des péridotites d'Oman. PhD thesis (Univ. Montpellier).

Noël, J., Godard, M., Oliot, E., Martinez, I., Williams, M., Boudier, F., Rodriguez, O., Chaduteaub, C., Escario, S., Gouze, P., 2018. Evidence of polygenetic carbon trapping in the Oman Ophiolite: Petro-structural, geochemical, and carbon and oxygen isotope study of the Wadi Dima harzburgite-hosted carbonates (Wadi Tayin massif, Sultanate of Oman). Lithos, 323:218-237.

Nolan, S.C., Skelton, P.W., Clissold, B.P., Smewing, J.D., 1990. Maastrichtian to early Tertiary stratigraphy and palaeogeography of the Central and Northern Oman Mountains. Geol. Soc. Special Pub., 49:495-519.

Oeser, M., Strauss, H., Wolff, P.E., Koepke, J., Peters, M., Garbe-Schönberg, D., Dietrich, M., 2012. A profile of multiple sulfur isotopes through the Oman ophiolite. Chem. Geol., 312:27-42.

Paukert, A.N., Matter, J.M., Kelemen, P.B., Shock, E.L., Havig, J.R., 2012. Reaction path modeling of enhanced in situ CO_2 mineralization for carbon sequestration in the peridotite of the Samail Ophiolite, Sultanate of Oman. Chem. Geol., 330-331:86-100.

Paukert Vankeuren, A., Matter, J.M., Stute, M., Kelemen, P.B., 2019. Multitracer determination of apparent groundwater ages in peridotite aquifers within the Samail Ophiolite, Sultanate of Oman. Earth Planet Sci. Lett., 516:37-48.

Rempfert, K.R., Miller, H.M., Bompard, N., Nothaft, D., Matter, J.M., Kelemen, P., Fierer, N., Templeton, A.S., 2017. Geological and geochemical controls on subsurface microbial life in the Samail Ophiolite, Oman. Frontiers in Microbiology, 56.

Rospabé, M., Benoit, M., Ceuleneer, G., Hodel, F., Kaczmarek, M.-A., 2018. Extreme geochemical variability through the dunitic transition zone of the Oman ophiolite: Implications for melt/fluid-rock reactions at Moho level beneath oceanic spreading centers. Geochim. Cosmochim. Acta, 234:1-23.

Rospabé, M., Ceuleneer, G., Benoit, M., Abily, B., Pinet, P., 2017. Origin of the dunitic mantle-crust transition zone in the Oman ophiolite: The interplay between percolating magmas and high temperature hydrous fluids. Geology, 45:471-474.

Snow, J.E., and Dick, H.J.B. 1995. Pervasive magnesium loss by marine weathering of peridotite. Geochim. Cosmochim. Acta, 59:4219-4235.

Streit, E., Kelemen, P., Eiler, J., 2012. Coexisting serpentine and quartz from carbonate-bearing serpentinized peridotite in the Samail Ophiolite, Oman. Contrib. Mineral. Petrol., 164:821-837.

Tamura, A., and Arai, S., 2006. Harzburgite-dunite-orthopyroxenite suite as a record of supra-subduction zone setting for the Oman ophiolite mantle. Lithos, 90:43-56.

VanTongeren, J.A., Hirth, G., Kelemen, P.B., 2015. Constraints on the accretion of the gabbroic lower oceanic crust from plagioclase lattice preferred orientations in the Samail ophiolite. Earth Planet. Sci. Lett., 427:249-261.

VanTongeren, J.A., Kelemen, P.B., Hanghoj, K., 2008. Cooling rates in the lower crust of the Oman ophiolite: Ca in olivine, revisited. Earth Planet. Sci. Lett., 267:69-82.

Figure F1. Geographical map of the Ibra-Wadi Tayin region, Oman, illustrating the location of places named in the text.

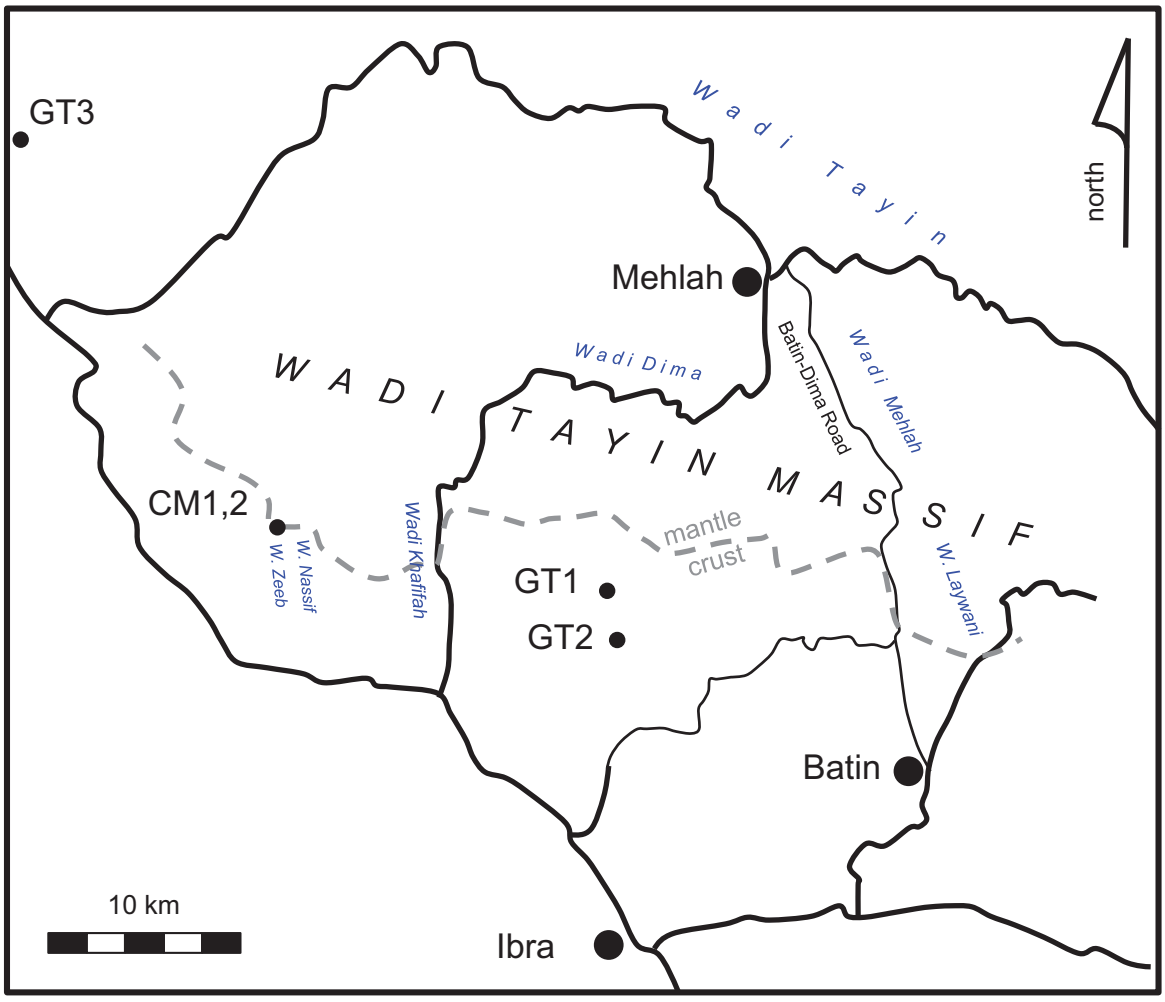

Figure F2. Geologic map of the eastern part of the Wadi Tayin massif of the Samail ophiolite, modified, with gratitude, from Noël et al. (2018) and Godard et al. (2019) with locations of the BA drill sites. **A.** Regional geology, with red line indicating position of cross-section in Figure F3. **B.** Detailed geologic observations near the drill sites.

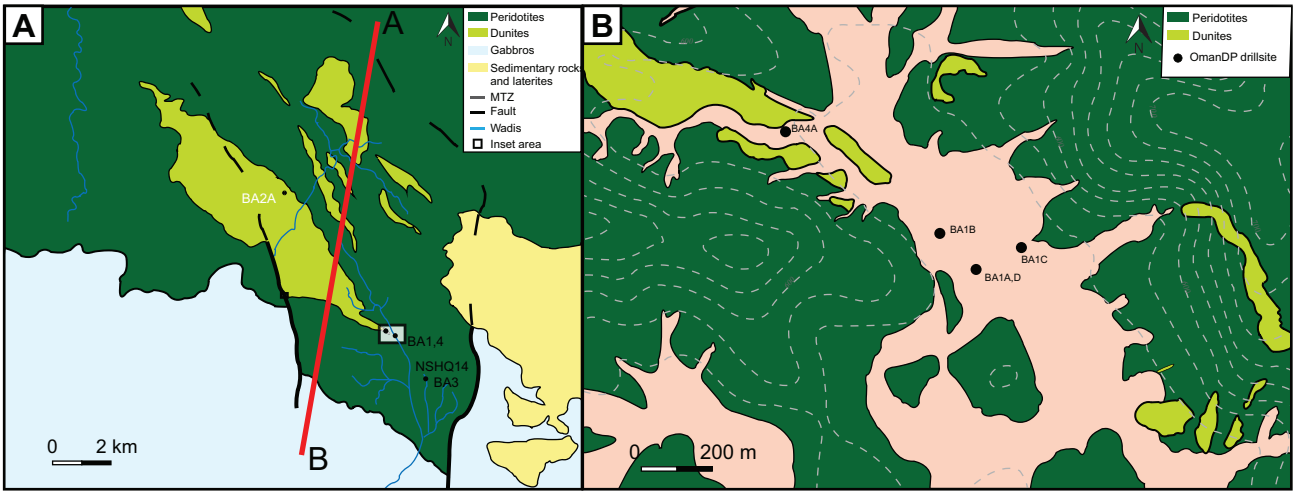

Figure F3. Cross-section of the eastern part of the Wadi Tayin massif of the Samail ophiolite. Location of the line of section is shown in Figure F2A (red line).

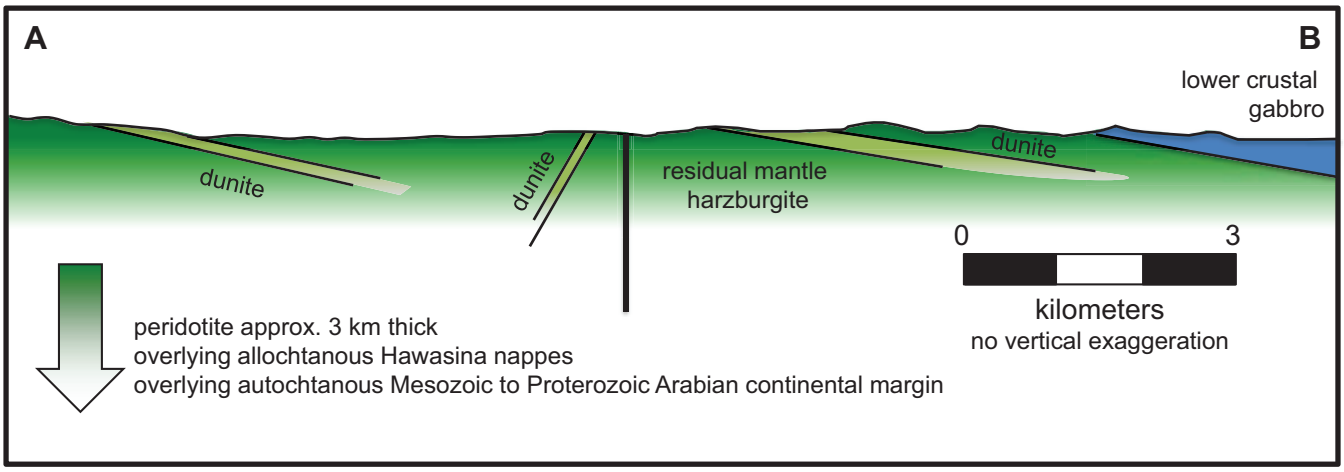

Tables

Table T1. Bulk XRD results from rotary hole samples, Holes BA1A and BA2A. **This table is available in Microsoft Excel format.**

Table T2. XRF data from Plymouth University, Holes BA1A and BA2A. **This table is available in Microsoft Excel format.**

Table T3. XRF standards and correction factors. **This table is available in Microsoft Excel format.**

Table T4. XRF and CIPW norms on cuttings, run at Sultan Qaboos University (SQU) and corrected per Table T3, Holes CA1C, BA1D, CM1B, and CM2A. **This table is available in Microsoft Excel format.**